Biotechnology Reports 36 (2022) e00766

Contents lists available at ScienceDirect

Biotechnology Reports

journal homepage: www.elsevier.com/locate/btre

Research Article

Quality evaluation of cell spheroids for transplantation by monitoring oxygen consumption using an on-chip electrochemical device

Mari Tsujimura [a], Kosuke Kusamori [a,*], Kodai Takamura [a], Temmei Ito [b], Takatoshi Kaya [b], Kazunori Shimizu [c], Satoshi Konishi [d], Makiya Nishikawa [a]

[a] Laboratory of Biopharmaceutics, Faculty of Pharmaceutical Sciences, Tokyo University of Science, 2641 Yamazaki, Noda, Chiba, 278-8510, Japan
[b] KONICA MINOLTA, INC., No.1 Sakura-machi, Hino-shi, Tokyo, 191-8511, Japan
[c] Department of Biomolecular Engineering, Graduate School of Engineering, Nagoya University, Furo-cho, Chikusa-ku, Nagoya, Aichi, 464-8603, Japan
[d] Department of Mechanical Engineering, Graduate School of Science and Engineering, Ritsumeikan University, 1-1-1 Noji-higashi, Kusatsu, Shiga, 525-8577, Japan

ARTICLE INFO

Keywords:
Cell-based therapy
Cell spheroid
Quality evaluation
Oxygen consumption
On-chip electrochemical device

ABSTRACT

Three-dimensional cell spheroids are superior cell-administration form for cell-based therapy which generally exhibit superior functionality and long-term survival after transplantation. Here, we nondestructively measured the oxygen consumption rate of cell spheroids using an on-chip electrochemical device (OECD) and examined whether this rate can be used as a marker to estimate the quality of cell spheroids. Cell spheroids containing NanoLuc luciferase-expressing mouse mesenchymal stem cell line C3H10T1/2 (C3H10T1/2/Nluc) were prepared. Spheroids of high or low quality were prepared by altering the medium change frequency. After transplantation into mice, the high-quality C3H10T1/2/Nluc spheroids exhibited a higher survival rate than the low-quality ones. The oxygen consumption rate of the high-quality C3H10T1/2/Nluc spheroids was maintained at high levels, whereas that of the low-quality spheroids decreased with time. These results indicate that OECD-based measurement of the oxygen consumption rate can be used to estimate the quality of cell spheroids without destructive analysis of the spheroids.

Abbreviations

ANOVA	Analysis of variance
DMEM	Dulbecco's modified Eagle's medium
FBS	Fetal bovine serum
HEPES	4-(2-hydroxyethyl)-1-piperazineethanesulfonic acid
JSPS	Japan Society for the Promotion of Science
LPS	Lipopolysaccharide
Nluc	NanoLuc luciferase
OECD	On-chip electrochemical device

1. Introduction

Cell-based therapy is a highly promising and effective method for treating refractory diseases, including diabetes, kidney diseases, and myocardial or nerve disorders. Furthermore, a single administration of therapeutic cells can show long-term therapeutic effects, unlike conventional drug therapies [1–4]. Despite this potential advantage, some serious problems have been identified for cell-based therapy, including the short-term survival and suboptimal function of transplanted cells. As these problems result in insufficient therapeutic outcomes, numerous attempts have been made to improve the survival and function of the transplanted cells [5–8]. Cell spheroids are three-dimensional cell structures that exhibit *in vivo*-like cell function [9, 10]. This is mainly because cells in cell spheroids, unlike monolayer-cultured cells, are under conditions of high cell–cell interactions, which induce *in vivo*-like gene and protein expression [11, 12]. Recently, several researchers, including our group, have demonstrated the usefulness of cell spheroids in cell-based therapies [13–15]. In our previous studies, cell spheroids composed of insulin-secreting cells reduced blood glucose level after transplantation in a diabetic mouse model and showed therapeutic effects superior to cell suspensions [16]. Furthermore, spheroids made of murine adipose-derived mesenchymal stem cell line m17.ASC showed an increased therapeutic effect in lipopolysaccharide (LPS)-induced inflammation model mice compared to cell suspension [17]. Thus, cell spheroids are expected to be clinically applied soon to solve problems associated with cell-based therapy.

The therapeutic application of cell spheroids requires quality control

* Corresponding author.
E-mail address: kusamori@rs.tus.ac.jp (K. Kusamori).

https://doi.org/10.1016/j.btre.2022.e00766
Received 5 August 2022; Received in revised form 19 September 2022; Accepted 1 October 2022
Available online 3 October 2022

Table 1
The size of spheroids. Results are expressed as mean ± SD of 100 experiments.

Seeding cell number ($\times 10^5$ cells)	Diameter (μm)
2	103 ± 16
5	141 ± 23
10	164 ± 21
20	253 ± 22

because the characteristics of cell spheroids depend on the preparation method, spheroid size, and culture time. Some spheroid preparation methods cannot control spheroid size and do not allow medium changes during spheroid culture [18–21]. These drawbacks of spheroid preparation methods have been largely solved by the recent advances in micromolding techniques. Microdevices developed using this technique can be used to prepare uniform-sized cell spheroids with appropriate medium-change intervals [22, 23]. Despite these advances, the quality of cell spheroids varies depending on culture and storage conditions. For effective and reproducible cell-based therapy using cell spheroids, the quality of the cell spheroids must be evaluated prior to transplantation.

Oxygen consumption is one of the most basic biological activities of cells and is strongly related to the function and survival of cells. To date, various methods have been developed to measure the oxygen consumption rate or metabolism of cells, including spectrophotometric, fluorescence, electrochemical, and photoluminescence techniques [24–26]. These techniques can help determine the biological activities of cells and can also be used for evaluating cell quality. However, these methods are generally complicated and require specialized techniques. More importantly, it is difficult to maintain intact cell spheroids after measuring the oxygen consumption rate. Therefore, these techniques are not suitable for facile quality evaluation of cell spheroids prior to transplantation.

An on-chip electrochemical device (OECD) contains biosensors for the electrochemical analysis of various chemicals, including DNA and oxygen [27]. To measure the oxygen consumption rate of cells, the integrated electrode array optimized for measuring oxygen enables the determination of the oxygen consumption rate of cultured cells, including monolayered cells or embryos (e.g., inhomogeneous blastocysts), with a single measurement. In recent years, OECDs have been improved to be easy to operate and to nondestructively measure the oxygen consumption rate of cells in a short time [28, 29]. Therefore, OECDs may be used to evaluate the quality of cell spheroids prior to transplantation.

In this study, we attempted to demonstrate the utility of OECDs for evaluating the quality of cell spheroids via measuring their oxygen consumption rate. To achieve this aim, cell spheroids under either good or bad conditions were prepared using the NanoLuc luciferase (Nluc)-expressing mouse mesenchymal stem cell line (C3H10T1/2/Nluc) by altering the medium-change frequency. Parameters related to the quality of the cell spheroids, including the oxygen consumption rate, were measured and compared with the survival rate of C3H10T1/2/Nluc spheroids post-transplantation.

2. Materials and methods

2.1. Animals

Male C3H/He mice (5 weeks old) were purchased from Sankyo Labo Service Co. Inc. (Tokyo, Japan) and were maintained under specific pathogen-free conditions. The protocols for experiments involving animals were approved by the Institutional Animal Experimentation Committee of Tokyo University of Science. All experiments involving animals were performed in accordance with the procedures outlined in the National Institutes of Health Guide for the Care and Use of Laboratory Animals and ARRIVE guidelines. In all experiments, mice were treated under isoflurane anesthesia and were euthanized by isoflurane over-inhalation after the experiments.

2.2. Materials

Hygromycin B Gold was purchased from InvivoGen Co. (San Diego, CA, USA). HEPES was purchased from Dojindo Laboratories (Kumamoto, Japan). Hank's balanced salt solution was purchased from Sigma-Aldrich (St. Louis, MO, USA). Deoxyribonuclease I from bovine pancreas, precrystalline, DISPASE II, NP-40 substrate, tris (hydroxymethyl) aminomethane, sodium deoxycholate, sodium dodecyl sulfate, chloroform, isopropyl alcohol, ethanol, $NaHCO_3$, d-(+)-glucose, and 0.4 w/v % trypan blue solution were purchased from FUJIFILM Wako Pure Chemical Co. (Osaka, Japan). Collagenase D was purchased from Roche Diagnostics, Inc. (Mannheim, Germany). Fetal bovine serum (FBS) was purchased from Biosera (East Sussex, UK). Dulbecco's modified Eagle's medium (DMEM) was purchased from Nissui Pharmaceutical Co. Ltd. (Tokyo, Japan). Mitomycin C, a penicillin-streptomycin-glutamine mixed solution, and 100 mM sodium pyruvate solution (100 ×) were purchased from Nacalai Tesque Inc. (Kyoto, Japan). All the other chemicals used were of the highest commercially available grade.

2.3. Cell culture

C3H10T1/2 cells were kindly provided by Dr. Hiroki Kagawa (Department of Cell Biology, Kyoto Pharmaceutical University, Kyoto, Japan) and were cultured in DMEM supplemented with 15% heat-inactivated FBS and penicillin-streptomycin-glutamine mixed solution at 37°C in a humidified air atmosphere containing 5% CO_2. C3H10T1/2/Nluc cells, established in our previous study [30], were cultured in the same medium containing 500 μg/mL hygromycin B.

2.4. Preparation of an agarose-based microwell sheet

Micropillar arrays and microwell sheets were fabricated as described previously [17]. Briefly, agarose was dissolved in ultrapure water to a final concentration of 3% (w/v) and heated in a microwave oven. The agarose solution was then poured onto the micropillar arrays and left for 20 min at room temperature (approximately 22°C). After gelation of the agarose solution, the agarose-based microwell sheet was detached from the micropillar arrays and cut to the size of a 6-well cell culture plate. The microwell sheets were placed in 6-well cell culture plates, washed with PBS, and sterilized with ultraviolet irradiation prior to cell seeding. Specifically, each microwell in an agarose-based microwell sheet has approximately 200 μm depth and approximately 500 μm width, and the sheet has 900 microwells.

2.5. Preparation of C3H10T1/2/Nluc spheroids

C3H10T1/2/Nluc cells were added at cell numbers of 2×10^5, 5×10^5, 1×10^6 and 2×10^6 onto the agarose-based microwell sheet set in 6-well culture plates. The culture plates were shaken for 1 h at 60 rpm in a CO_2 incubator, and the culture medium was changed. During the following experimental period, the culture medium of "the medium-change group" was changed every 24 h, and the medium of "the no medium-change group" was kept unchanged. C3H10T1/2/Nluc spheroids collected from the microwell sheets were observed under a BZ-9000 microscope, and the diameter was measured using BZ-9000 analyzer software. The cell number per spheroid was counted after dispersing the spheroids using a digestion solution (0.05 g of collagenase D, 0.05 g of DNase I and 0.3 g of dispase II in 100 ml of 1 × PBS) as previously described [31] followed by staining with a trypan blue solution.

2.6. Measurement of luciferase activity of C3H10T1/2/Nluc spheroids

C3H10T1/2/Nluc spheroids were dispersed for 15–30 min at 37°C using a digestion solution and the dispersed cells were centrifuged at

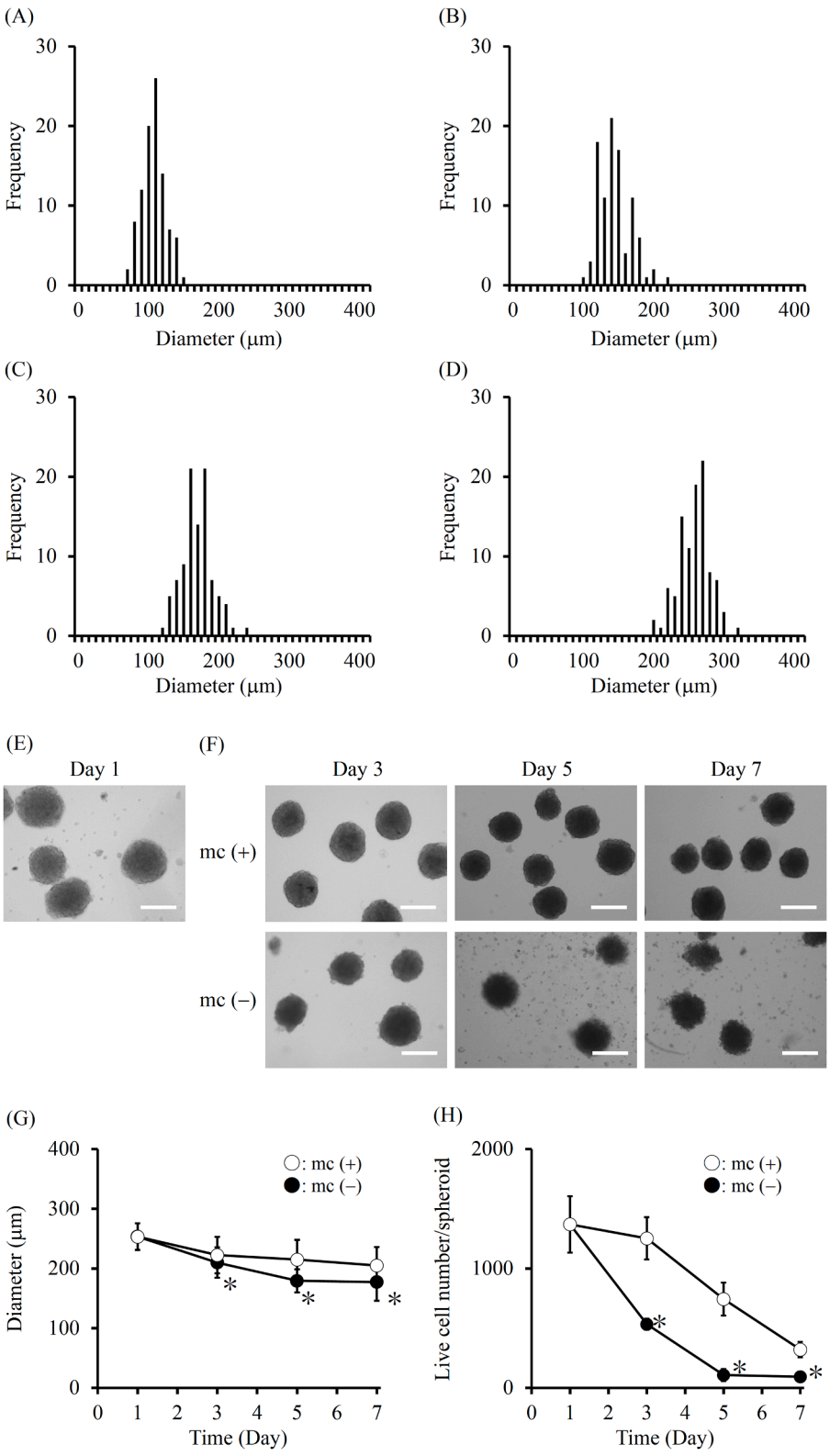

Fig. 1. Characteristics of C3H10T1/2/Nluc spheroids. Diameter histogram of C3H10T1/2/Nluc spheroids with varying seeded cell numbers: (A) 2×10^5, (B) 5×10^5, (C) 1×10^6 or (D) 2×10^6 cells/well. The results are expressed as the mean ± SD of 100 samples. Representative images of two independent experiments with similar results are shown. (E, F) Typical images of C3H10T1/2/Nluc spheroids with or without medium changes every 24 h. The groups with medium change (mc (+)) and without medium change (mc (−)) are indicated. Representative images of two independent experiments with similar results are shown. Scale bars represent 200 μm. (G) Change in diameter of C3H10T1/2/Nluc spheroids with or without medium change every 24 h. The groups with medium change (mc (+)) and without medium change (mc (−)) are indicated. The results are expressed as the mean ± SD of 100 (mc (+)) or 47 (mc (−)) samples. Representative images of two independent experiments with similar results are shown. *$p < 0.05$, statistically significant differences were observed in comparison with the medium-change group at the same time point. (H) Number of C3H10T1/2/Nluc spheroids with or without medium change every 24 h. The groups with medium change (mc (+)) and without medium change (mc (−)) are indicated. The results are expressed as the mean ± SD of three to five samples. Representative images of three independent experiments with similar results are shown. *$p < 0.05$, statistically significant differences were observed in comparison with the medium-change group at the same time point.

150 × *g* for 3 min. The supernatant was then removed, and the cells were lysed with lysis buffer (20 mM Tris-HCl, 200 mM NaCl, 2.5 mM $MgCl_2$, 0.05 w/v% NP-40, pH7.4). The luciferase activity of the cells was measured by detecting the luminescence using Nano-Glo assay reagent (Promega Co., Tokyo, Japan), and luminescence was measured using the EnVision multi-label plate reader (Perkin-Elmer, Wellesley, MA, USA). C3H10T1/2/Nluc spheroids were seeded into a 96-well culture plate and cultured for 24 h in a CO_2 incubator. The medium was collected and luciferase activity in the medium was measured as described above.

2.7. Survival of C3H10T1/2/Nluc spheroids after transplantation into mice

C3H10T1/2/Nluc spheroids were prepared as described above by

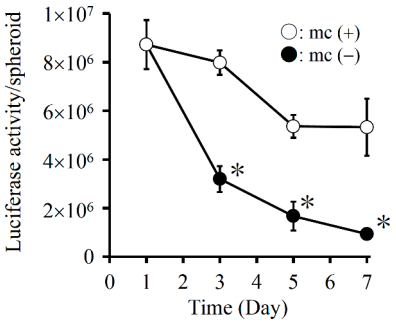

Fig. 2. Luciferase activity of C3H10T1/2/Nluc spheroids.
Luciferase activity of the C3H10T1/2/Nluc spheroids with or without medium change every 24 h. The groups of medium change (mc (+)) and without medium change (mc (−)) are indicated. Results are expressed as the mean ± SD of three to five samples. Representative of three independent experiments with similar results is shown. *p < 0.05, statistically significant differences observed in comparison with the medium change group at the same time point.

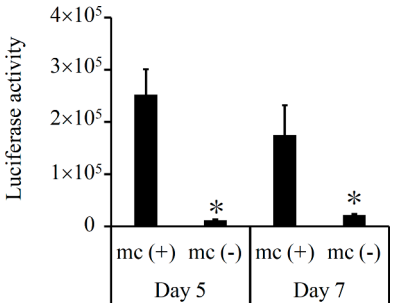

Fig. 3. Survival rate after transplantation of C3H10T1/2/Nluc spheroids.
Survival rate after transplantation of C3H10T1/2/Nluc spheroids with or without medium change every 24 h. The groups with medium change (mc (+)) and without medium change (mc (−)) are indicated. The results are expressed as the mean ± SD of three to four samples. Representative images of two independent experiments with similar results are shown. ns, not significant; *p < 0.05, statistically significant differences observed in comparison with the medium-change group at the same time point.

adding 2 × 10^6 cells to each well. Twenty C3H10T1/2/Nluc spheroids were subcutaneously transplanted into the backs of C3H/He mice under isoflurane anesthesia. The mice were sacrificed 5 h after cell transplantation by isoflurane over-inhalation, and the tissue at the transplantation site was collected and homogenized in lysis buffer using a homogenizer (Microtec, Chiba, Japan). The homogenate was then centrifuged at 10,000 × *g* for 10 min at 4°C. Luciferase activity in the supernatant was evaluated as previously described.

2.8. Device fabrication

The OECD system includes a chip sensor, a measuring device, a temperature controller, and a sensor plate fixture (Supplementary Figure 1). The chip sensor was produced using semiconductor process technology. The working electrode chip consists of a micropit and Pt electrodes. Pt rings electrodes were fabricated in the following process; First, Pt rings were fabricated on a SiO_2/Si substrate using Ti/Pt sputtering and a dry etching. Next, thin SiO_2 layer was fabricated on the Ti/Pt layer by sputtering. Subsequently, the SiO_2 layer in the designated areas were removed by wet etching, exposing eight Pt disks (5 μm in diameter) in each Pt ring pattern. The counter and reference electrodes consist of Pt disk electrodes and insulation layers consists of SiO_2 layer. This chip device consists of 6 wells, one well for measuring reference and counter currents. A micropit (200 μm diameter and 80 μm depth) was fabricated at the center of the chip for the settling of a spheroid. Disk electrodes were regularly placed from the edge of the micropits (20, 70, 120, 200, 300 and 400 μm distance for 200 μm micropit), and eight microelectrodes were placed on each disk electrode.

2.9. Measurement of oxygen consumption rate of cell spheroids

As previously reported [28], this system uses the principle of electrochemical detection of the oxygen concentration around the cell by electrodes and conversion of electrode output into oxygen consumption (Supplementary Figure 2). The spherical diffusion theory was used for general analysis of the oxygen consumption rate of the cell spheroids. The measurement program was optimized by setting sufficient waiting time until the oxygen-consuming layer was formed by the spheroids. When measuring spheroids with 200 μm sensor, spheroids were visually confirmed to be settled down in the center of the micropit and the nearest electrode from the edge of micropit (20 μm) was not used for calculating oxygen consumption rate due to possibility of contacting cell spheroid and electrode.

The measuring plate contained a chip sensor and was filled with 2 mL of culture medium containing 25 mM HEPES buffer. After filling the measurement medium, -0.6 and +0.05 V square wave pulses were applied to each electrode for 14 cycles per 2 s until the oxygen reduction current curve was uniformly stable. After running this cycle for 8 min to stabilize the sensor, a -0.6 V pulse was applied to each chip for 4 s, and the oxygen reduction current was collected as the background. The C3H10T1/2/Nluc spheroids were then transferred to each micropit using a micropipette, and a measurement voltage of -0.6 V was applied for 2 min to measure the oxygen consumption rate.

2.10. Mitomycin C treatment of C3H10T1/2/Nluc spheroids

Mitomycin C was used to inhibit DNA replication by cross-linking it with double-stranded DNA. C3H10T1/2/Nluc spheroids were prepared as described above by adding 2 × 10^6 cells to each well. The spheroids were cultured in a medium containing 50 or 100 μg/mL mitomycin C for 24 h, and the oxygen consumption rate of C3H10T1/2/Nluc spheroids was measured by the OECD as described above. The concentration of mitomycin C was determined by confirming its effect on the oxygen consumption rate of spheroids in a preliminary study.

2.11. Evaluation of proliferation of C3H10T1/2/Nluc spheroids after measurement of the oxygen consumption rate

C3H10T1/2/Nluc spheroids were prepared as described above by adding 2 × 10^6 cells to each well. After measurement of the oxygen consumption rate by the OECD, C3H10T1/2/Nluc spheroids were re-seeded into a 96-well culture plate and cultured for 24 h in a CO_2 incubator. The proliferation of cells in the C3H10T1/2/Nluc spheroids was measured using the Cell Counting Kit-8 (Dojindo Laboratories).

2.12. Statistical analysis

Statistical differences were evaluated using one-way analysis of variance (ANOVA) followed by Student's *t*-test for two groups. Statistical significance was set at $p < 0.05$.

3. Results

3.1. Characteristics of C3H10T1/2/Nluc spheroids

The characteristics of microwell sheets have already been reported [17]. C3H10T1/2/Nluc spheroids of different sizes were prepared depending on the number of cells added to the microwell sheets (Table 1, Figs. 1A-D). In the following experiments, those with the largest size were used to evaluate the influence of medium change on the characteristics of C3H10T1/2/Nluc spheroids. The spherical shape and

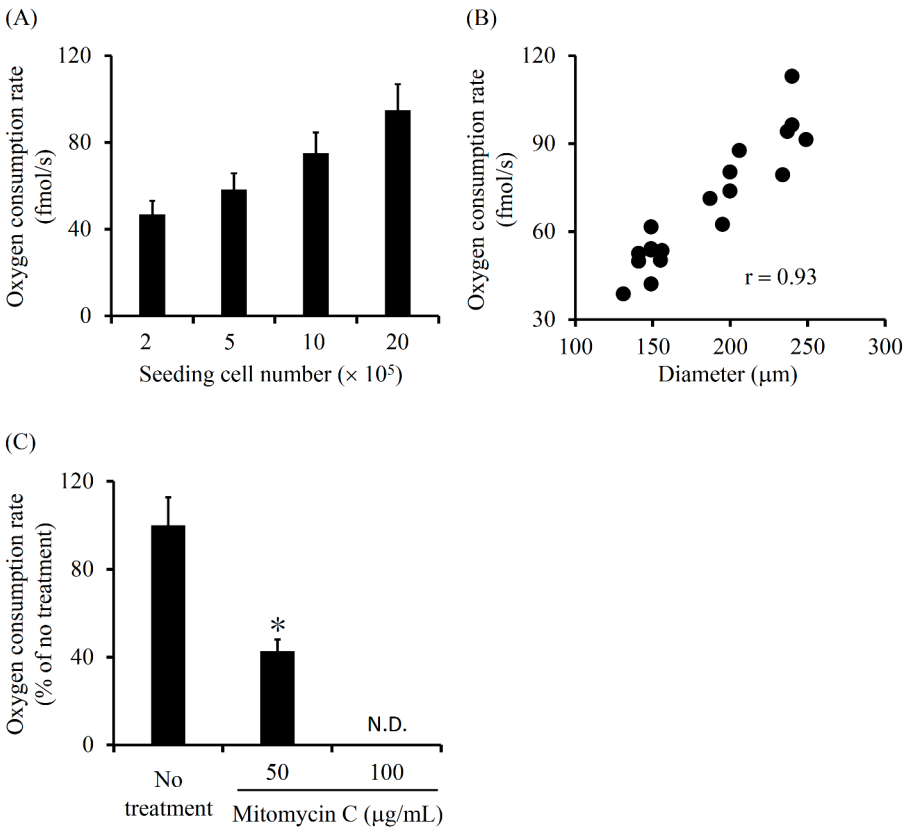

Fig. 4. Oxygen consumption rate of C3H10T1/2/Nluc spheroids.
(A) Oxygen consumption rate of C3H10T1/2/Nluc spheroids with varying seeded cell number. Results are expressed as the mean ± SD of five samples. Representative of two independent experiments with similar results is shown. (B) The correlation coefficient between the oxygen consumption rate and the diameter of cell spheroids. (C) Oxygen consumption rate of cell spheroids treated with mitomycin C. Results are expressed as the mean ± SD of five samples. Representative of two independent experiments with similar results is shown. *p < 0.05, statistically significant differences observed in comparison with no treatment group. N.D., not detected.

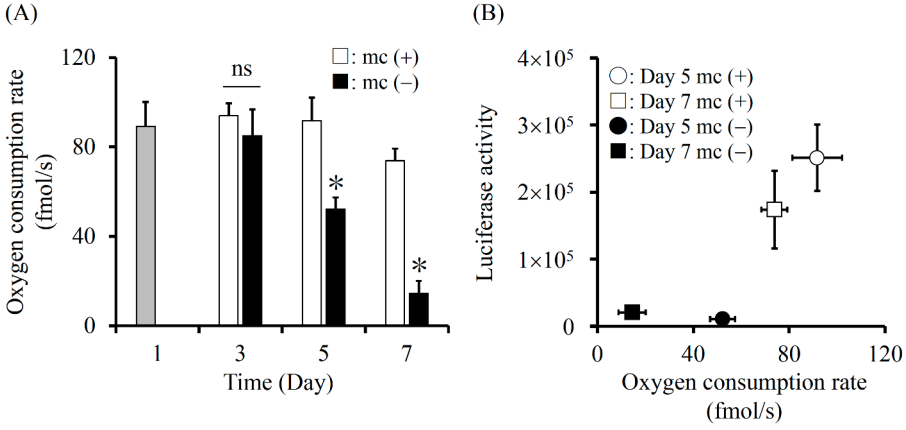

Fig. 5. Correlation between oxygen consumption rate and luciferase activity after transplantation of C3H10T1/2/Nluc spheroids.
(A) Oxygen consumption rate of C3H10T1/2/Nluc spheroids with or without medium change every 24 h. The groups of medium change (mc (+)) and without medium change (mc (−)) are indicated. Results are expressed as the mean ± SD of four or five samples. Representative of three independent experiments with similar results is shown. ns, not significant; *p < 0.05, statistically significant differences observed in comparison with the medium-change group at the same time point. (B) The correlation between oxygen consumption rate and luciferase activity after transplantation of C3H10T1/2/Nluc spheroids. Day 5 mc (+) (white circle), Day 7 mc (+) (white square), Day 5 mc (−) (black circle), and Day 7 mc (−) (black square) are indicated. Results are expressed as the mean ± SD of three or four samples. A representative of two independent experiments with similar results is shown.

size of the C3H10T1/2/Nluc spheroids remained almost unchanged during the experimental period of 168 h after daily medium change. In contrast, without daily medium change, the surfaces of the spheroids became rough, and their size decreased with time (Figs. 1E-G). In addition, the number of live cells in the no medium-change group was significantly lower than that in the medium-change group on day 3 and thereafter (Fig. 1H). These results indicate that no medium change greatly reduced the quality of C3H10T1/2/Nluc spheroids.

3.2. Luciferase activity of C3H10T1/2/Nluc spheroids

To quantitatively evaluate the quality of the C3H10T1/2/Nluc spheroids, their intracellular luciferase activities was measured. The intracellular luciferase activities decreased with time in both groups (Fig. 2), and consistent with the results in Fig. 1H, the activity of the no medium-change group was significantly lower than that of the medium change group. These results indicated that the luciferase activity of the spheroids can be used as an indicator of cell quality in C3H10T1/2/Nluc spheroids. In subsequent experiments, the quality of the spheroids was evaluated based on intracellular luciferase activity.

3.3. Survival rate after transplantation of C3H10T1/2/Nluc spheroids into mice

To evaluate the survival of C3H10T1/2/Nluc spheroids prepared by 5- or 7-day culture with or without medium change, these cells were subcutaneously transplanted into the back of C3H/He mice. Based on the results of a preliminary experiments, the survival of the spheroids

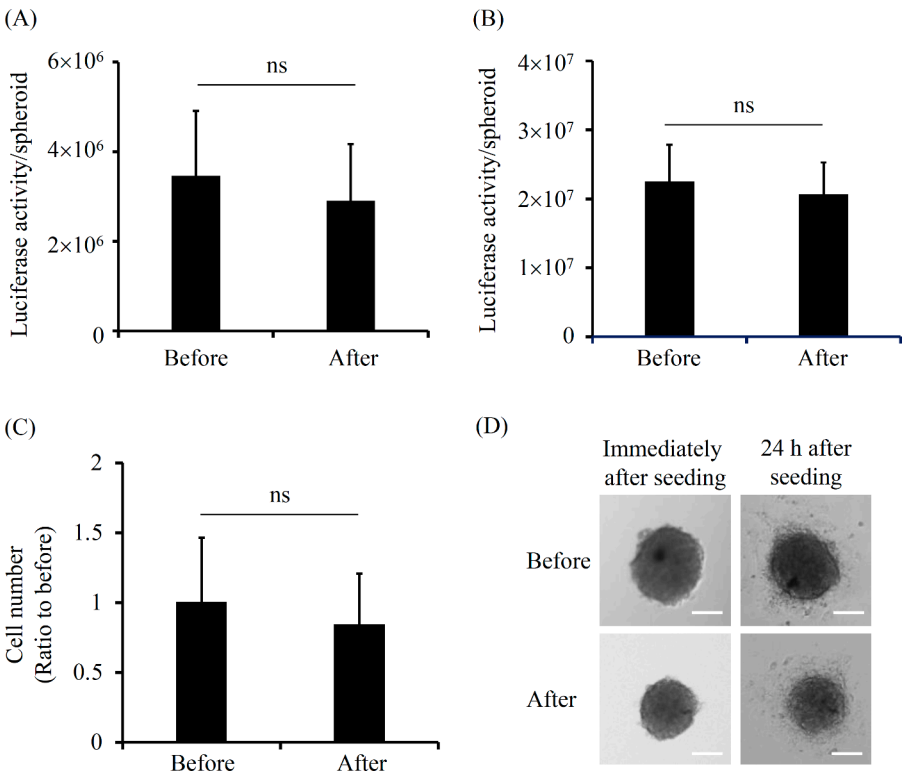

Fig. 6. Characteristics of C3H10T1/2/Nluc spheroids after the measurement of oxygen consumption rate. (A) The luciferase activity of C3H10T1/2/Nluc spheroids after measurement of the oxygen consumption rate. Before and after groups indicate the luciferase activity before or after measurement of the oxygen consumption rate using the OECD, respectively. Representative of two independent experiments with similar results is shown. Results are expressed as the mean ± SD of five samples. ns, not significant. (B) The luciferase activity of secreted from C3H10T1/2/Nluc spheroids after measurement of oxygen consumption rate. Before and after groups indicate the luciferase activity before or after measurement of the oxygen consumption rate using the OECD, respectively. Representative of two independent experiments with similar results is shown. Results are expressed as the mean ± SD of twenty samples. ns, not significant. (C) The proliferation of C3H10T1/2/Nluc spheroids after measurement of the oxygen consumption rate. Before and after groups indicate the proliferation before or after measurement of oxygen consumption rate using OECD, respectively. Representative of two independent experiments with similar results is shown. Results are expressed as the mean ± SD of five samples. ns, not significant. (D) Typical images of C3H10T1/2/Nluc spheroids after 24 h of measurement of oxygen consumption rate. Before and after groups indicate the images before and after measurement of oxygen consumption rate using OECD, respectively. Representative of five independent experiments with similar results is shown. Scale bars represent 100 μm.

was evaluated 5 h after transplantation. The survival rate of the 5- and 7-day culture C3H10T1/2/Nluc spheroids was significantly higher in the medium-change group than in the no medium-change group (Fig. 3).

3.4. Oxygen consumption rate of C3H10T1/2/Nluc spheroids

The oxygen consumption rate of C3H10T1/2/Nluc spheroids prepared under various conditions was measured by OECD. The oxygen consumption rate of C3H10T1/2/Nluc spheroids depended on the number of cells seeded on the microwell sheets (Fig. 4A). The oxygen consumption rate and diameter of the spheroids were well correlated with a correlation coefficient of 0.93 (Fig. 4B). The oxygen consumption rate of C3H10T1/2/Nluc spheroids treated with mitomycin C was measured to evaluate the effect of cell viability on the oxygen consumption rate. Thus, the oxygen consumption rate of C3H10T1/2/Nluc spheroids decreased when incubated with mitomycin C-containing culture medium (Fig. 4C).

3.5. Correlation between oxygen consumption rate and luciferase activity after transplantation of C3H10T1/2/Nluc spheroids

To evaluate the correlation between the oxygen consumption rate and the survival rate after transplantation of C3H10T1/2/Nluc spheroids, the oxygen consumption rate of C3H10T1/2/Nluc spheroids was measured under various conditions. The oxygen consumption rate of the no medium-change group decreased with culture time (Fig. 5A), and the rate of 5- or 7-day culture spheroids of the no medium-change group was significantly lower than that of the medium-change group. In addition, the oxygen consumption rates of the 5- and 7-day culture C3H10T1/2/Nluc spheroids were plotted against the luciferase activity after transplantation into mice, and a positive correlation was observed when the oxygen consumption is 40 fmol/s or more (Fig. 5B).

3.6. Influence of the measurement of oxygen consumption rate on the characteristics of C3H10T1/2/Nluc spheroids

The luciferase activity of C3H10T1/2 spheroids was measured before and after measuring the oxygen consumption rate of the spheroids. The measurement had little effect on the intercellular and extracellular luciferase activities of the spheroids (Figs. 6A,B). Similar results were obtained for proliferation and adhesion of C3H10T1/2/Nluc spheroids (Fig. 6C,D). These results indicate that the measurement is not only a nondestructive method but has little influence on the characteristics of spheroids.

4. Discussion

The quality of pharmaceuticals in the market must be strictly controlled for effective and safe use in clinical practice. However, this is not the case for cellular pharmaceuticals. The heterogeneity of cells may cause unstable cell function and survival [32–34], and effective and reproducible cell-based therapy cannot be achieved. Therefore, the development of a method to nondestructively evaluate the quality of cells prior to transplantation into patients is necessary for the realization of excellent cell-based therapy. Cell spheroids potentially have high functionality because of firm and multiple cell–cell interactions. Therefore, cell spheroids have been reported to show higher therapeutic effects after transplantation than cell suspensions [16, 17, 35, 36]. In this study, the quality of cell spheroids was evaluated before transplantation to realize highly effective and reproducible cell-based therapy using cell spheroids of guaranteed high quality.

The OECD is an on-chip device that enables nondestructive measurement of the oxygen consumption rate of cells. OECD has been used to measure the oxygen consumption rate of human embryos [27–29]. The rate changed depending on embryo proliferation. However, another study reported that the oxygen consumption rate of embryos did not correlate with their transplantation rate [37]. The embryos were divided into high (14.71 ± 4.61 fmol/s) and low oxygen consumption rate (7.65

± 1.50 fmol/s) groups, and their transplantation rates were 56.6 and 70.0%, respectively, which were not significantly different from each other. Despite these results, attention should be paid to whether the oxygen consumption rate was accurately measured because the rates measured were very low, even in the high oxygen consumption rate group. Therefore, in this study, we evaluated whether the device could sensitively measure the oxygen consumption rate of cell spheroids. We then examined whether the rate was a suitable index for the selection of high-quality cell spheroids for transplantation.

We showed that the oxygen consumption rate of the cell spheroid increased as the viable cell number of the spheroids increased, and we confirmed that the viable cell number of cell spheroids could be evaluated from the oxygen consumption rate measured using the OECD. In fact, in *in vitro* experiments using mitomycin C, the oxygen consumption rate of the C3H10T1/2 cell spheroids decreased according to the concentration of mitomycin C, which decreased the number of viable cells (Fig. 4C). Furthermore, the measurement of the oxygen consumption rate by OECD hardly affected the survival and function of cells forming the cell spheroids (Figs. 6A-D). In the present study, cell spheroids of good or poor quality were prepared by changing the medium change frequency. These results indicate that the oxygen consumption rate measured using the OECD can be used to predict the transplantation efficiency of cell spheroids of varying qualities. The results of this study raise the possibility that cell spheroids can be screened by measuring the oxygen consumption rate using the OECD prior to transplantation to realize highly effective and reproducible cell-based therapy.

5. Conclusions

The oxygen consumption rate of cell spheroids measured using OECDs can be used to evaluate the quality of cell spheroids for transplantation, and the OECD-based quality check of cell spheroids will lead to excellent cell-based therapy with high-quality cell spheroids.

Funding

This work was supported in part by a Grant-in-Aid for Scientific Research (C) (grant number 20K12653) and Fostering Joint International Research (B) (grant number 21KK0200) from the Japan Society for the Promotion of Science (JSPS), an Adaptable and Seamless Technology Transfer Program through a Target-driven R&D grant (grant number JPMJTM20LJ) from the Japan Science and Technology Agency, and by a GSK Japan Research Grant 2017.

Data availability

Data will be made available on request.

Declaration of Competing Interest

The authors declare no competing interests.

Data Availability

No data was used for the research described in the article.

Acknowledgements

The authors are grateful to Editage (www.editage.com) for English language editing.

Supplementary materials

Supplementary material associated with this article can be found, in the online version, at doi:10.1016/j.btre.2022.e00766.

References

[1] AM Shapiro, M Pokrywczynska, C. Ricordi, Clinical pancreatic islet transplantation, Nat. Rev. Endocrinol. 13 (5) (2017) 268–277, https://doi.org/10.1016/j.nbt.2022.06.005.
[2] D Liu, F Cheng, S Pan, Z. Liu, Stem cells: a potential treatment option for kidney diseases, Stem Cell Res. Ther. 11 (2020) 249, https://doi.org/10.1186/s13287-020-01751-2.
[3] R Guo, M Morimatsu, T Feng, F Lan, D Chang, F Wan, Y. Ling, Stem cell-derived cell sheet transplantation for heart tissue repair in myocardial infarction, Stem Cell Res. Ther. 11 (2020) 19, https://doi.org/10.1186/s13287-019-1536-y.
[4] L Jiang, S Jones, X. Jia, Stem cell transplantation for peripheral nerve regeneration: current options and opportunities, Int. J. Mol. Sci. 18 (2017) 94, https://doi.org/10.3390/ijms18010094.
[5] Rocco GD BaldariS, M Piccoli, M Pozzobon, M Muraca, G. Toietta, Challenges and strategies for improving the regenerative effects of mesenchymal stromal cell-based therapies, Int. J. Mol. Sci. 18 (2017) 2087, https://doi.org/10.3390/ijms18102087.
[6] A Trounson, C. McDonald, Stem cell therapies in clinical trials: progress and phallenges, Cell Stem Cell 17 (2015) 11–22, https://doi.org/10.1016/j.stem.2015.06.007.
[7] IB Copland, J Galipeau, Death and inflammation following somatic cell transplantation, Semin. Immunopathol. 33 (2011) 535–550, https://doi.org/10.1007/s00281-011-0274-8.
[8] AS Lee, M Inayathullah, MA Lijkwan, X Zhao, W Sun, S Park, et al., Prolonged survival of transplanted stem cells after ischaemic injury via the slow release of pro-survival peptides from a collagen matrix, Nat. Biomed. Eng. 2 (2018) 104–113, https://doi.org/10.1038/s41551-018-0191-4.
[9] A. Abbott, Cell culture: biology's new dimension, Nature 424 (2003) 870–872, https://doi.org/10.1038/424870a.
[10] TM Achilli, J Meyer, JR. Morgan, Advances in the formation, use and understanding of multi-cellular spheroids, Expert Opin. Biol. Ther. 12 (2012) 1347–1360, https://doi.org/10.1517/14712598.2012.707181.
[11] RZ Lin, HY. Chang, Recent advances in three-dimensional multicellular spheroid culture for biomedical research, Biotechnol. J. 3 (2008) 1172–1184, https://doi.org/10.1002/biot.200700228.
[12] E Fennema, N Rivron, J Rouwkema, C van Blitterswijk, J. de Boer, Spheroid culture as a tool for creating 3D complex tissues, Trends Biotechnol. 31 (2013) 108–115, https://doi.org/10.1016/j.tibtech.2012.12.003.
[13] K Kusamori, M Nishikawa, N Mizuno, T Nishikawa, A Masuzawa, Y Tanaka, et al., Increased insulin secretion from insulin-secreting cells by construction of mixed multicellular spheroids, Pharm. Res. 33 (2016) 247–256, https://doi.org/10.1007/s11095-015-1783-2.
[14] CS Ong, X Zhou, J Han, CY Huang, A Nashed, S Khatri, et al., In vivo therapeutic applications of cell spheroids, Biotechnol. Adv. 36 (2018) 494–505, https://doi.org/10.1016/j.biotechadv.2018.02.003.
[15] C Rathnam, L Yang, S Castro-Pedrido, J Luo, L Cai, KB. Lee, Hybrid SMART spheroids to enhance stem cell therapy for CNS injuries, Sci. Adv. 7 (2021) eabj2281, https://doi.org/10.1126/sciadv.abj2281.
[16] K Kusamori, M Nishikawa, N Mizuno, T Nishikawa, A Masuzawa, K Shimizu, et al., Transplantation of insulin-secreting multicellular spheroids for the treatment of type 1 diabetes in mice, J. Control Release 10 (2014) 119–124, https://doi.org/10.1016/j.jconrel.2013.10.024.
[17] Y Shimazawa, K Kusamori, M Tsujimura, A Shimomura, R Takasaki, Y Takayama, et al., Intravenous injection of mesenchymal stem cell spheroids improves the pulmonary delivery and prolongs in vivo survival, Biotechnol. J. 17 (2022), e2100137, https://doi.org/10.1002/biot.202100137.
[18] J Landry, D Bernier, C Ouellet, R Goyette, N. Marceau, Spheroidal aggregate culture of rat liver cells: histotypic reorganization, biomatrix deposition, and maintenance of functional activities, J. Cell Biol. 101 (1985) 914–923, https://doi.org/10.1083/jcb.101.3.914.
[19] JM Yuhas, AP Li, AO Martinez, AJ. Ladman, A simplified method for production and growth of multicellular tumor spheroids, Cancer Res. 37 (1977) 3639–3643.
[20] JM Kelm, NE Timmins, CJ Brown, M Fussenegger, LK. Nielsen, Method for generation of homogeneous multicellular tumor spheroids applicable to a wide variety of cell types, Biotechnol. Bioeng. 83 (2003) 173–180, https://doi.org/10.1002/bit.10655.
[21] H Song, O David, S Clejan, CL Giordano, H Pappas-Lebeau, L Xu, et al., Spatial composition of prostate cancer spheroids in mixed and static cultures, Tissue Eng. 10 (2004) 1266–1276, https://doi.org/10.1089/ten.2004.10.1266.
[22] AP Napolitano, P Chai, DM Dean, JR. Morgan, Dynamics of the self-assembly of complex cellular aggregates on micromolded nonadhesive hydrogels, Tissue Eng. 13 (2007) 2087–2094, https://doi.org/10.1089/ten.2006.0190.
[23] A Khademhosseini, R. Langer, Microengineered hydrogels for tissue engineering, Biomaterials 28 (2007) 5087–5092, https://doi.org/10.1016/j.biomaterials.2007.07.021.
[24] PR Territo, RS. Balaban, Rapid spectrophotometric determination of oxygen consumption using hemoglobin, in vitro: light scatter correction and expanded dynamic range, Anal. Biochem. 286 (2000) 156–163, https://doi.org/10.1006/abio.2000.4774.
[25] C Diepart, J Verrax, PB Calderon, O Feron, BF Jordan, B. Gallez, Comparison of methods for measuring oxygen consumption in tumor cells in vitro, Anal. Biochem. 396 (2010) 250–256, https://doi.org/10.1016/j.ab.2009.09.029.

[26] R Obregon, Y Horiguchi, T Arai, S Abe, Y Zhou, R Takahashi, et al., A Pt layer/Pt disk electrode configuration to evaluate respiration and alkaline phosphatase activities of mouse embryoid bodies, Talanta 94 (2012) 30–35, https://doi.org/10.1016/j.talanta.2012.01.059.
[27] Y Date, S Takano, H Shiku, K Ino, T Ito-Sasaki, M Yokoo, et al., Monitoring oxygen consumption of single mouse embryos using an integrated electrochemical microdevice, Biosens. Bioelectron. 30 (2011) 100–106, https://doi.org/10.1016/j.bios.2011.08.037.
[28] H Kurosawa, H Utsunomiya, N Shiga, A Takahashi, M Ihara, M Ishibashi, et al., Development of a new clinically applicable device for embryo evaluation which measures embryo oxygen consumption, Hum. Reprod. 31 (2016) 2321–2330, https://doi.org/10.1093/humrep/dew187.
[29] K Hiramoto, M Yasumi, H Ushio, A Shunori, K Ino, H Shiku, et al., Development of oxygen consumption analysis with an on-chip electrochemical device and simulation, Anal. Chem. 89 (2017) 10303–10310, https://doi.org/10.1021/acs.analchem.7b02074.
[30] M Tsujimura, K Kusamori, H Katsumi, T Sakane, A Yamamoto, M. Nishikawa, Cell-based interferon gene therapy using proliferation-controllable, interferon-releasing mesenchymal stem cells, Sci. Rep. 9 (2019) 18869, https://doi.org/10.1038/s41598-019-55269-6.
[31] B Weigmann, I Tubbe, D Seidel, A Nicolaev, C Becker, MF. Neurath, Isolation and subsequent analysis of murine lamina propria mononuclear cells from colonic tissue, Nat. Protoc. 2 (2007) 2307–2311, https://doi.org/10.1038/nprot.2007.315.
[32] LA Costa, N Eiro, M Fraile, LO Gonzalez, J Saá, P Garcia-Portabella, et al., Functional heterogeneity of mesenchymal stem cells from natural niches to culture conditions: implications for further clinical uses, Cell. Mol. Life Sci. 7 (2021) 447–467, https://doi.org/10.1007/s00018-020-03600-0.
[33] J Epah, R. Schäfer, Implications of hematopoietic stem cells heterogeneity for gene therapies, Gene Ther. 28 (2021) 528–541, https://doi.org/10.1038/s41434-021-00229-x.
[34] YY Lipsitz, NE Timmins, PW. Zandstra, Quality cell therapy manufacturing by design, Nat. Biotechnol. 34 (2016) 393–400, https://doi.org/10.1038/nbt.3525.
[35] NH Lee, O Bayaraa, Z Zechu, HS. Kim, Biomaterials-assisted spheroid engineering for regenerative therapy, BMB Rep. 54 (2021) 356–367, https://doi.org/10.5483/BMBRep.2021.54.7.059.
[36] Y Petrenko, E Syková, Š. Kubinová, The therapeutic potential of three-dimensional multipotent mesenchymal stromal cell spheroids, Stem Cell Res. Ther. 8 (2017) 94, https://doi.org/10.1186/s13287-017-0558-6.
[37] T Kuno, M Tachibana, A Fujimine-Sato, M Fue, K Higashi, A Takahashi, et al., A preclinical evaluation towards the clinical application of oxygen consumption measurement by CERMs by a mouse chimera model, Int. J. Mol. Sci. 20 (2019) 5650, https://doi.org/10.3390/ijms20225650.